HEWLETT-PACKARD COMPANY
Intellectual Property Administration
P. O. Box 272400
Fort Collins, Colorado 80527-2400

IDW AF

PATENT APPLICATION

ATTORNEY DOCKET NO. 10004618-1

IN THE
UNITED STATES PATENT AND TRADEMARK OFFICE

Inventor(s): Yong Chen

Confirmation No.: 6205

Application No.: 09/815,913

Examiner: Olsen, Allen W

Filing Date: Mar. 22, 2001

Group Art Unit: 1763

Title: SCANNING PROBE BASED LITHOGRAPHIC ALIGNMENT

Mail Stop AF
Commissioner for Patents
PO Box 1450
Alexandria, VA 22313-1450

TRANSMITTAL LETTER FOR RESPONSE/AMENDMENT

Sir:

Transmitted herewith is/are the following in the above-identified application:

(X) Response/Amendment
( ) New fee as calculated below
(X) No additional fee
( ) Other: _____ (fee $_____)
( ) Petition to extend time to respond
( ) Supplemental Declaration

CLAIMS AS AMENDED BY OTHER THAN A SMALL ENTITY						
(1) FOR	(2) CLAIMS REMAINING AFTER AMENDMENT	(3) NUMBER EXTRA	(4) HIGHEST NUMBER PREVIOUSLY PAID FOR	(5) PRESENT EXTRA	(6) RATE	(7) ADDITIONAL FEES
TOTAL CLAIMS		MINUS		= 0	X $18	$ 0
INDEP. CLAIMS		MINUS		= 0	X $88	$ 0
[ ] FIRST PRESENTATION OF A MULTIPLE DEPENDENT CLAIM					+ $300	$ 0
EXTENSION FEE	1ST MONTH $110.00 [ ]	2ND MONTH $430.00 [ ]	3RD MONTH $980.00 [ ]	4TH MONTH $1530.00 [ ]		$ 0
					OTHER FEES	$
					TOTAL ADDITIONAL FEE FOR THIS AMENDMENT	$ 0

Charge $ 0 to Deposit Account 08-2025. At any time during the pendency of this application, please charge any fees required or credit any overpayment to Deposit Account 08-2025 pursuant to 37 CFR 1.25. Additionally please charge any fees to Deposit Account 08-2025 under 37 CFR 1.16 through 1.21 inclusive, and any other sections in Title 37 of the Code of Federal Regulations that may regulate fees. A duplicate copy of this sheet is enclosed.

I hereby certify that this correspondence is being deposited with the United States Postal Service as first class mail in an envelope addressed to: Commissioner for Patents, Alexandria, VA 22313-1450.

Date of Deposit: **Oct. 25, 2004**

Typed Name: **Edouard Garcia**

Signature: _____

Respectfully submitted,

Yong Chen

By _____

Edouard Garcia

Attorney/Agent for Applicant(s)
Reg. No. **38,461**

Date: **Oct. 25, 2004**

Telephone No.: **(650) 631-6591**

Rev 10/04 (TransAmd)

- Attach as First Page to Transmitted Papers -

Attorney's Docket No.: 10004618-1

IN THE UNITED STATES PATENT AND TRADEMARK OFFICE

Applicant : Yong Chen
Serial No. : 09/815,913
Filed : March 22, 2001
Title : SCANNING PROBE BASED LITHOGRAPHIC ALIGNMENT

Art Unit : 1763
Examiner : Olsen, Allen W

Commissioner for Patents
P.O. Box 1450
Alexandria, VA 22313-1450

RESPONSE TO THE EXAMINER'S ACTION DATED AUGUST 24, 2004

I. Status of claims

Claims 1-21 are pending. Claims 3 and 11-21 have been withdrawn from consideration.

II. Claim rejections under 35 U.S.C. § 103

The Examiner has rejected claims 1, 2, and 4-10 under 35 U.S.C. § 103(a) over Chou (U.S. 5,772,905) in view of Samsavar (U.S. 5,866,806).

A. The Examiner has failed to establish a proper *prima facie* case of obviousness

For the purpose of the following discussion, the examiner is reminded that:

> To establish a *prima facie* case of obviousness, three basic criteria must be met. First, there must be some suggestion or motivation, either in the references themselves or in the knowledge generally available to one of ordinary skill in the art, to modify the references or to combine reference teachings. Second, there must be a reasonable expectation of success.

CERTIFICATE OF MAILING

I hereby certify that this correspondence is being deposited with the United States Postal Service as First Class Mail in an envelope addressed to: Commission for Patents, PO Box 1450, Alexandria, VA 22313-1450 on:

October 25, 2004
Date

(Signature of person mailing papers)

Edouard Garcia
(Typed or printed name of person mailing papers)

> Finally, the prior art reference (or references when combined) must teach or suggest all the claim limitations. The teaching or suggestion to make the claimed combination and the reasonable expectation of success must both be found in the prior art, and not on applicants' disclosure.

MPEP § 706.02(j) (emphasis added).

The Examiner has argued repeatedly that (emphasis added):

> It would have been obvious to one skilled in the art to measure tunneling current to align the mold and substrate of Chou because Chou teaches capacitance sensing as an electrical alignment technique and Samsavar teaches that the measurement of capacitance and the measurement of tunneling current may both be used to determine the relative proximity or alignment between two features. As such, capacitance and tunneling current measurements are recognized in the art as equivalent means for determining the alignment of two features.

With this rejection, however, the Examiner has failed to provide the requisite factual basis and failed to establish the requisite motivation to support his deemed conclusion that the features recited in claims 1, 2, and 4-10 would have been obvious to one of ordinary skill in the art at the time the invention was made. Indeed, the Examiner has failed to meet each of the three requirements for a proper *prima* facie case of obviousness listed under MPEP § 706.02(j):

1. The Examiner has failed to point to any teaching or suggestion to operate Chou's system in the manner proposed by the Examiner

First, Samsavar's teaching that a scanning probe tip can be used to locate an exposed surface feature either by sensing changes in tunneling current or capacitance does not constitute a teaching or suggestion "to measure tunneling current to align the mold and substrate" using Chou's nanoimprint lithography system, as asserted by the Examiner. Indeed, as explained in detail below, it is not possible to observe any tunneling current using Chou's nanoimprint lithography system.

In Chou's system, the alignment marks 64, 68 are respectively covered by the silicon dioxide mold layer 14 and the thermoplastic polymer layer 20. Consequently, during the alignment process, the alignment marks 64, 68 are separated by at least the combined

thickness of the silicon dioxide mold layer 14 and the thermoplastic polymer layer 20. Chou teaches that the silicon dioxide mold layer 14 has a thickness of at least 5-200 nm (col. 4, lines 42-43) and that the thermoplastic polymer layer 20 has a thickness of 50-250 nm (col. 4, lines 58-59). Thus, the minimal separation distance between the alignment marks 64, 68 during the alignment process would be at least 55 nm. For a tunneling current to be observed, however, the distance between the alignment marks must be less than a few nanometers (nm) so that the electron clouds (or wavefunctions) between the alignment marks overlap (see, e.g., the highlighted sections on pages 2 and 5 of the portion of the Thesis by Matthew Ellis that is attached hereto; also see the Background section of U.S. Patent No. 4,724, 318, which is referenced at col. 3, line 66 of Samsavar and is attached hereto).

In addition, as evidenced by the highlighted section on page 13 of the attached Thesis by Matthew Ellis, the tunneling effect also requires a tunneling probe that has an extremely small radius of curvature at the tip (i.e., of atomic or near atomic sharpness). Neither of the alignment marks 64, 68 in Chou's system has an extremely small radius of curvature at the tip.

For these reasons, contrary to the Examiner's assumption, no observable tunneling current could possibly be measured between the alignment marks 64, 68 in Chou's nanoimprint lithography system because the separation distance between the alignment marks 64, 68 during the alignment process is too great and because neither alignment mark 64, 68 has a tip feature with the requisite tip sharpness.

2. The Examiner has failed to explain how one of ordinary skill in the art could have reasonably expected to measure tunneling current between the alignment marks in Chou's system

Second, the Examiner has failed to address the issue of whether one of ordinary skill in the art at the time the invention was made would have had a reasonable expectation of successfully measuring a tunneling current between the alignment marks 64, 68 in Chou's nanoimprint lithography system.

3. The Examiner's proposed modification of Chou's system would not teach or suggest all the claim limitations

Third, the Examiner's proposal to use Chou's system "to measure tunneling current to align the mold and substrate" does not teach or suggest all of the elements recited in the claims. In particular, the alignment marks 64, 68 in Chou's system are capacitor plates (see col. 6, line 61); neither of the alignment marks 64, 68 includes a scanning probe. Therefore, Chou's system cannot align a patterned mold with respect to an alignment mark disposed on a substrate based upon interaction of a scanning probe with the alignment mark, as recited in claims 1, 2, and 4-10.

4. Conclusion

Without a proper explanation for combining the teachings of Chou and Samsavar to arrive at the inventive method recited in claims 1, 2, and 4-10, the Examiner has failed to establish a proper *prima facie* case of obviousness and, therefore, the rejection of claims 1, 2, and 4-10 under 35 U.S.C. § 103(a) over Chou in view of Samsavar should be withdrawn.

B. It would not have been obvious to combine the teachings of Chou and Samsavar as proposed by the Examiner

The Examiner has asserted that "it would have been obvious to one skilled in the art to measure tunneling current to align the mold and substrate of Chou." As explained above, however, no observable tunneling current could possibly be measured between the alignment marks 64, 68 in Chou's nanoimprint lithography system because the separation distance between the alignment marks 64, 68 during the alignment process is too great and because neither alignment mark 64, 68 has a tip feature with the requisite tip sharpness.

Since it is not physically possible to measure a tunneling current between the alignment marks 64, 68 of Chou's nanoimprint lithography system during the alignment process, one of ordinary skill in the art clearly would not have been motivated "to measure tunneling current to align the mold and substrate of Chou," as asserted by the Examiner. For this additional reason, the Examiner's rejection of claims 1, 2, and 4-10 under 35 U.S.C. § 103(a) over Chou in view of Samsavar should be withdrawn.

C. The teachings of Chou and Samsavar do not render the claimed invention obvious

No permissible combination of Chou and Samsavar would have led one of ordinary skill in the art to modify the method described in Chou to arrive at the inventive lithographic method recited in claims 1, 2 and 4-10.

The scan probe tip 26 and sensor 24 described in Samsavar are capable of measuring certain properties of a surface, such as tunneling current, capacitance, magnetic force, van der Waals forces, and electrical resistance (see, e.g., col. 3, line 66 through col. 4, line 2). In Samsavar's approach, the scan probe tip 26 either contacts the surface of interest or is spaced apart from the surface of interest by an air gap. Samsavar does not teach or suggest that the scan probe tip 26 is capable of measuring the above-mentioned properties of a surface through a layer of solid material, much less though a silicon dioxide mold layer 14 and a thermoplastic polymer layer 20 having a minimal combined separation distance of at least 55 nm. Consequently, there is no teaching or suggestion in Samsavar that would have led one of ordinary skill in the art at the time the invention was made to have a reasonable expectation that the substitution of Samsavar's scan probe tip 26 for the mold alignment mark 64 would have resulted in a system capable of successfully measuring a tunneling current. To the contrary, as explained above, the minimal separation distance of 55 nm that is achievable with Chou's approach would prevent any tunneling current from being observed during the mold alignment process. Thus, one of ordinary skill in the art would have been led away from such a modification of Chou's system.

Some additional, non-trivial modification of Chou's nanoimprint lithography system would have been required to arrive at a system capable of performing the inventive lithographic method recited in claims 1, 2, and 4-10. However, neither Chou nor Samsavar provides any teaching or suggestion that would have led one of ordinary skill in the art at the time of the invention to modify Chou's nanoimprint lithography in such a way.

Thus, neither Chou nor Samsavar provides any teaching or suggestion that would have led one of ordinary skill in the art to successfully modify Chou's nanoimprint lithographic system so that it could align a patterned mold with respect to an alignment mark disposed on a substrate based upon interaction of a scanning probe with the alignment mark, as recited in claims 1, 2 and 4-10. For this additional reason, the Examiner's rejection of

independent claims 1, 2, and 4-10 under 35 U.S.C. § 103(a) over Chou in view of Samsavar should be withdrawn.

III. Conclusion

For the reasons explained above, all of the pending claims are now in condition for allowance and should be allowed.

Charge any excess fees or apply any credits to Deposit Account No. 08-2025.

Respectfully submitted,

Date: October 25, 2004

Edouard Garcia
Reg. No. 38,461
Telephone No.: (650) 631-6591

Please direct all correspondence to:

Hewlett-Packard Company
Intellectual Property Administration
Legal Department, M/S 35
P.O. Box 272400
Fort Collins, CO 80528-9599

Selected Pages of a Thesis by Matthew Ellis

Texas Tech University

April 5, 1998

Published at http://www.phys.ttu.edu/~tlmde/thesis/TOC.html

INTRODUCTION

Invented in 1982 by Binnig and Rohrer[1], the scanning tunneling microscope (STM) was the first instrument to perform real space atomic resolution imaging of the surface of a material. The first success of this instrument was to resolve the debate concerning the surface reconstruction of the Si(111) surface.[2] Since then, the STM has become a very powerful tool for surface science. The success of the STM spawned an entire class of scanning probe microscopes and corresponding techniques. Scanning force microscopes such as the magnetic force microscope (MFM), the electrostatic force microscope (EFM), and the atomic force microscope (AFM), have been developed based on the STM. Many techniques such as scanning capacitance microscopy, scanning Kelvin microscopy, and scanning tunneling spectroscopy are now routinely employed via scanning probe microscopes for surface science.

Historical Development

The topografiner was the earliest instrument to resemble the STM in functionality. Using a piezoelectric drive system similar to the STM, this instrument scanned surfaces to obtain an image. Instead of using a tunneling current through a small potential barrier as the sensing mechanism, the topografiner used field emission for the electron source. Developed in the late 1960s by Young, Ward, and Scire, the topografiner scanned with the probe about 1000 Å from the surface. Applying a high voltage of a few kV created a field emission current. Using the field emission current intensity as the feedback signal created topographic images of the sample. The lateral resolution of this device was at best approximately 4000 Å. Young also used the topografiner to study vacuum tunneling. Early work in vacuum tunneling provided the theoretical basis for understanding the tunneling mechanism in scanning tunneling microscopy.

Operating Mechanism

The scanning tunneling microscope is essentially a very sensitive profilometer that uses quantum mechanical tunneling as the sensing method. A small metallic probe, usually made of tungsten or a platinum-iridium alloy, is scanned across a sample surface by piezoelectric transducers (Figure 1). These transducers provide motion in three orthogonal directions. A saw tooth waveform rasters the probe in the x-direction, while a

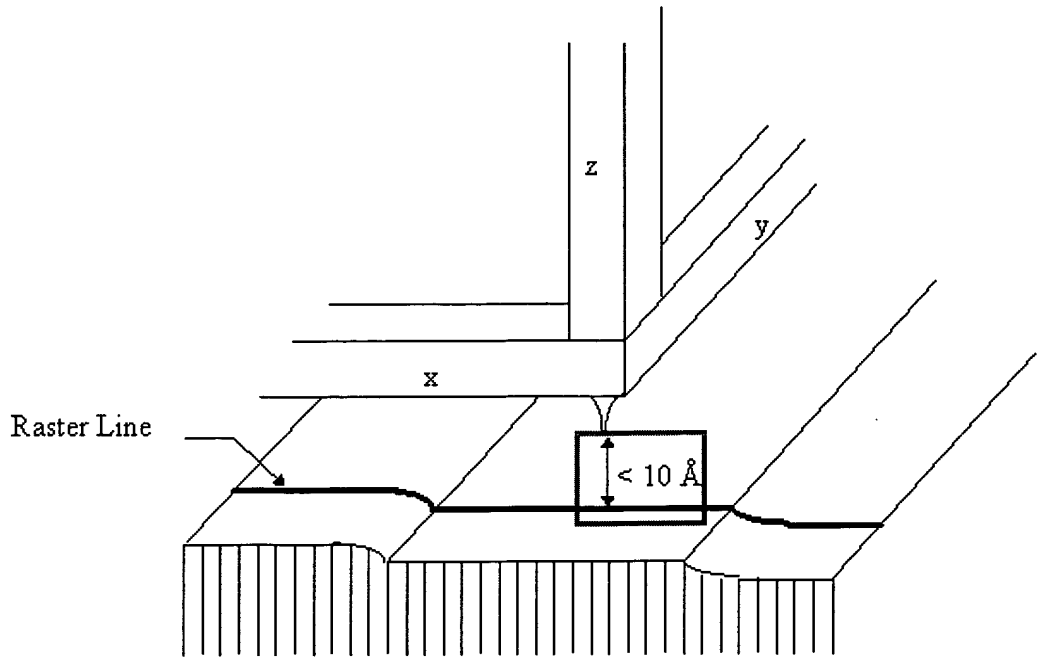

Figure 1

ramp voltage advances the raster signal in the y-direction. With this notation the probe-sample distance is on the z-axis. A third voltage adjusts this z distance so that the probe and sample remain separated by a few angstroms creating a small vacuum potential barrier.

Scanning a metal probe a few angstroms from a surface is usually impossible without some type of feedback and control system. A tunneling current across the vacuum barrier provides the input for such a feedback and control system. By overlapping the electron wavefunctions in the metallic probe and the sample, tunneling current flows when a bias is applied between the probe and sample. Amplifying this tunneling current and comparing it to a set point value creates a signal suitable for feedback on the voltage applied to the z piezoelectric transducer. This feedback loop created by the tunneling current and the z piezoelectric transducer voltage maintains a constant separation distance between the probe and the sample as scanning occurs, creating an array of z voltages that represent a contour plot of the sample.

Tunneling

Tunneling, a quantum mechanical phenomenon, creates the high degree of sensitivity necessary for atomic scale imaging of surfaces. Since the scanning tunneling microscope works by measuring the tunneling current between a sharp metal probe and a sample surface, a very simple model of vacuum tunneling between two metals can explain why the scanning tunneling microscope is so sensitive.

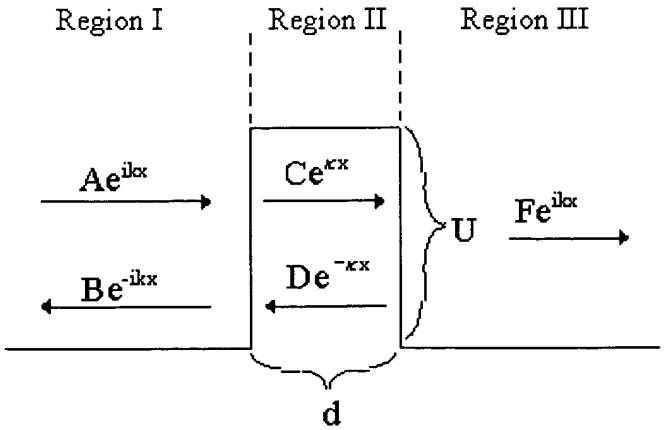

Figure 2

The standard one-dimensional square barrier problem in quantum mechanics shows the exponential current dependence on the probe-sample separation. Figure 2 shows a square energy barrier in one dimension with an electron wave packet originating from the left side of the barrier. The width of this barrier, d, roughly corresponds to the separation between the probe and sample. The barrier height, *U*, depends on many factors and is difficult to determine. In general, the Schrödinger equation for this situation is as follows:

$$\frac{p_x^2}{2m} + U(x) = E$$

$$-\frac{\hbar^2}{2m}\frac{\partial^2}{\partial x^2}\psi(x) + U(x)\psi(x) = E\psi(x)$$

Assuming the solution to equation 2 is of exponential form results in two cases. The first case, when the energy of the particle is greater than the barrier energy, we have an oscillating solution of the form:

$$\psi(x) = \psi(0)e^{\pm ikx}$$

$$k = \frac{\sqrt{2m(E-U)}}{\hbar}$$

The second case deals with the operational mode of the STM. In this situation, the energy of the particle is less than the energy of the barrier and the solutions are of the form:

$$\psi(x) = \psi(0)e^{-\kappa x}$$

$$\kappa = \frac{\sqrt{2m(U-E)}}{\hbar}$$

From this solution we can determine the probability for an electron crossing the barrier

$$P \propto |\psi_x(0)|^2 e^{-2\kappa x}$$

$$I \propto e^{-2\kappa d}$$

and find that the current is exponentially dependent on the distance between the probe and the sample.

Equation 8 shows that the tunneling current, *I*, is proportional to the exponential of separation distance d. The decay constant, κ , is proportional the square root of the difference between the barrier energy *U* and the electron energy *E*. The energy *E* is the energy of electrons in the Fermi level neglecting thermal excitation. The difference of *U* and *E* can be described as the work function φ . For many metals, the work function is approximately 4-5 eV, which makes the factor of 2κ approximately equal to 2Å^{-1}. Therefore, the tunneling current changes by almost an order or magnitude for every angstrom of vacuum between the electrodes. This extreme current sensitivity provides the basic means of measuring the sample surface.

Constant Height and Constant Current Imaging

As mentioned previously, to obtain a surface image the probe is scanned across the surface with feedback creating what is known as a "constant current" scan. For atomically smooth surfaces, the probe may be scanned across the surface with very slow feedback, allowing the tunneling current variations to determine the surface topography. This method is known as the "constant height" scan. Each method of obtaining images has advantages and disadvantages. Constant height scanning works well when slowly imaging small areas with small height variations. Problems with this approach stem from the inability to prevent the probe from crashing into large surface features on the sample. Constant current imaging can overcome this problem in many instances. Feedback from the tunneling current maintains a safe distance from the sample, allowing for fast scans over a rough surface. In either case, keeping a small metal probe within angstroms of a surface is a difficult problem with many challenges.

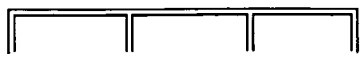

Previous Section	Table of Contents	Next Section
Email Matt	Matt's Home Page	April 5, 1998

ATOMIC SCALE TUNNELING AND IMAGING

The physical interaction used in obtaining the surface information for a scanning tunneling microscope is quantum mechanical tunneling. A brief and simplified discussion of tunneling through a vacuum barrier was given above. Now a more detailed examination of the tunneling mechanism follows. The simplest explanation of the scanning tunneling microscope as a very sensitive profilometer depends on the belief that at the atomic scale the STM is actually taking a surface profile of the sample. At an atomic scale the notion of surface topography is unclear. A simple assumption would be that surface topography at the atomic scale is a contour of the charge density of the surface material. Only electrons near the Fermi level contribute to the tunneling and all electrons below the Fermi level contribute to the charge density, so, assuming that the topography produced by changes in the tunneling current is a contour of the charge density may not be entirely correct.[3]

In addition to the uncertainty regarding the surface topography, the electron transport processes in an STM are different from the standard mechanism described as tunneling. Usually, the tunneling process has a barrier width of 20-30 angstroms; but in an STM, the barrier is only a few angstroms wide. Also, overlap between the surface potentials of the probe and sample may place the top of the potential barrier lower than that of the vacuum level.[4] Sometimes the potential barrier level is even lower than the Fermi level. The local atomic structure between the probe and the sample also play an important role in determining the current. Finally, many forces exist between the probe and the sample affecting the tunneling current.

Ballistic Transport and Tunneling

Atomic scale tunneling differs from conventional tunneling in one important aspect. The width of the potential barrier is small compared to that in usual discussions of tunneling. In fact, with a small enough barrier tunneling might not be an accurate description of the process occurring. Arguments invoking the uncertainty principle show that the location of the electron is unknown with respect to the barrier.[5] Thus, regarding atomic scale potential barriers the difference between the ballistic transport and tunneling is nonexistent. Two approaches with the uncertainty principle show this nondistinction.

The first approach shows the uncertainty of the electron energy, in the region of the barrier, is greater than its kinetic energy. Inside the region of the barrier, the electron has a velocity determined by its kinetic energy.

$$v = \sqrt{\frac{2(E - U_B)}{m}}$$

With this velocity, the time for an electron to pass through the barrier is:

$$\Delta t = d\sqrt{\frac{m}{2(E - U_B)}}$$

Using the energy-time uncertainty relation:

$$\Delta E \geq \frac{\hbar}{\Delta t} = \frac{\hbar}{d}\sqrt{\frac{2(E - U_B)}{m}}$$

Assuming $E\text{-}U_B$ = 3eV, and the barrier thickness is approximately 2 Å, the energy uncertainty, Δ E, is about 3.4 eV. Thus, the uncertainty of the energy is larger than the absolute value of the electron kinetic energy.

The second approach shows the uncertainty in position of an electron may be greater than the barrier thickness. The de Broglie wavelength of the electron in the classically allowed region of the barrier is given by equation 12.

$$\lambda = \frac{2m\hbar}{\sqrt{2m(E - U_B)}}$$

Given an electron with a kinetic energy of 3eV, the de Broglie wavelength of the electron is approximately 7.1 Å, which is the same order of magnitude as the barrier thickness.

Modeling the Tunneling Current

Regardless of the uncertainty relations given above, a tunneling Hamiltonian approach using first order perturbation theory may be used to calculate the tunneling current. Based on a method developed by Bardeen[6] for metal-insulator-metal tunneling junctions, this approach begins by considering two subsystems instead of attempting to analyze the Schrödinger equation of the combined system. For each subsystem, solving the stationary Schrödinger equation determines the electronic states. Then, using time dependent perturbation theory, the electron transfer rate between the electrodes may be found. The overlap of the surface wavefunctions of the two subsystems at a separation surface determines the amplitude of the electron transfer, also known as the tunneling matrix M. By modifying the wavefunctions of one surface due to the presence of the other, the Bardeen approach to tunneling may be applied to the tunneling in an STM. This method is also known as the modified Bardeen approach (MBA).[7]

Using this approach, the tunneling current is,

$$I = \frac{2me}{\hbar}\sum_{\mu\nu}\left\{f(E_\mu)\left[1 - f(E_\nu)\right] - f(E_\nu)\left[1 - f(E_\mu)\right]\right\}\left|M_{\mu\nu}\right|^2 \delta(E_\nu + V - E_\nu)$$

In this expression *f(E)* is the Fermi function, V is the applied voltage, and $M_{\mu\nu}$ is the tunneling matrix element between the state of the probe and the sample. Evaluating the tunneling matrix $M_{\mu\nu}$ is usually the most difficult step in determining the tunneling current. This difficulty stems from lack of knowledge of the probe and sample wavefunctions. If the probe and sample wavefunctions are known $M_{\mu\nu}$ can be evaluated using the expression developed by Bardeen

$$M_{\mu\nu} = -\frac{\hbar^2}{2m}\int_{\Sigma}\left(\chi_\nu^* \nabla \psi_\mu - \psi_\mu \nabla \chi_\nu^*\right) \bullet dS$$

Equation 14 determines the tunneling matrix $M_{\mu\nu}$. In this expression, χ_ν is the modified wavefunction for the probe and ψ_μ is the wavefunction for the sample. The integral is performed over the surface area defined by *S*.

Local Density of States (LDOS) Topography

Although the MBA model works reasonably well for a variety of conditions, this model requires knowledge of the wavefunction of the surface and the probe. As mentioned previously, these wavefunctions are usually not known, especially for the tunneling probe. Assuming a simple model for the probe, and using the first order perturbation theory for determining the tunneling current, leads to the conclusion that the tunneling current is proportional to the local density of states.

The simplest model of the probe is that it is a point source of current. Assuming the probe is a point source of current allows the analysis to determine properties of the sample only. In actual STM measurements, the probe and sample wavefunctions are responsible for the tunneling current. With the probe modeled as a mathematical point source of current, equation 13 for the current at small voltages reduces to[8]

$$I \propto \sum_{\nu} |\psi_{\mu}(r)|^2 \delta(E_{\mu} - E_F) \equiv \rho(r, E_F)$$

In this equation, E_F is the Fermi level of the sample surface, ψ_μ is the wavefunction for the surface at position r. The quantity $\rho(r,E_F)$ is the local density of states of the sample.

Lateral Resolution Models

Initial attempts to estimate the resolution of a scanning tunneling microscope showed that a very high resolution was possible with even a moderately sharp probe. The initial spherical probe model by Binnig, the s-wave model, and probe-sample interactions provide insight to the origin of atomic resolution in the scanning tunneling microscope.

One of the first estimates of the lateral resolution of the STM came from Binnig in 1978.[9] Assuming the tunneling probe was spherical in shape with a radius R, Binnig determined the tunneling current would be related to the probe radius by equation 16.

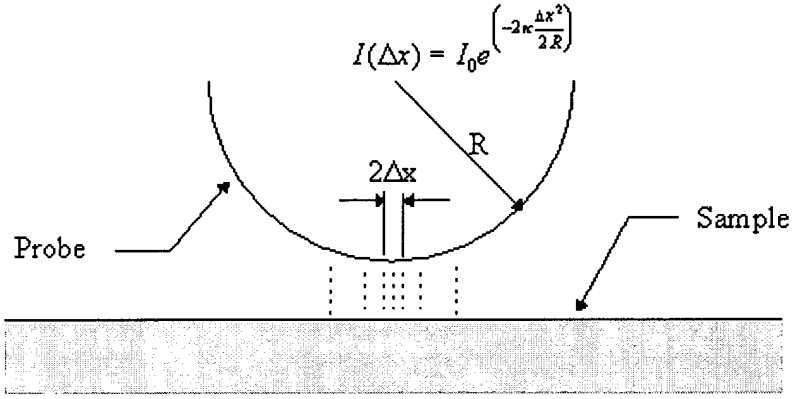

Figure 3

This equation is based on the idea that the probe radius is much larger than the distance between the probe and the surface. In this case the current lines are almost perpendicular to the sample surface (Figure 3).

With $\kappa \approx 1$ Å^{-1} and R$\approx$ 100 Å, the current concentrates in a small radius of approximately 14 Å; thus, the expected resolution should not exceed this value. Modern scanning tunneling microscopes routinely exceed this resolution. Thus, a more accurate model of the probe-sample interaction is necessary.

Soon after achieving atomic resolution with the STM, Tersoff and Hamann[10] proposed the s-wave model of probe sample interaction to account for the experimental results of Binnig and Rohrer. They modeled the probe as a protruded piece of Sommerfeld metal with a radius of curvature of R. The probe wavefunctions were then assumed to be solutions of the Schrödinger equation for a spherical potential well. Assuming only the s-wave solution was important, Tersoff and Hamann were led to a simple solution for the tunneling current. Under a low bias the s-wave model shows the tunneling current to be proportional to the Fermi level local density of states at the center of the curvature of the probe r_o (equation 17).

$$I \propto \sum_{E_o} |\psi_{\mu}(r_o)|^2$$

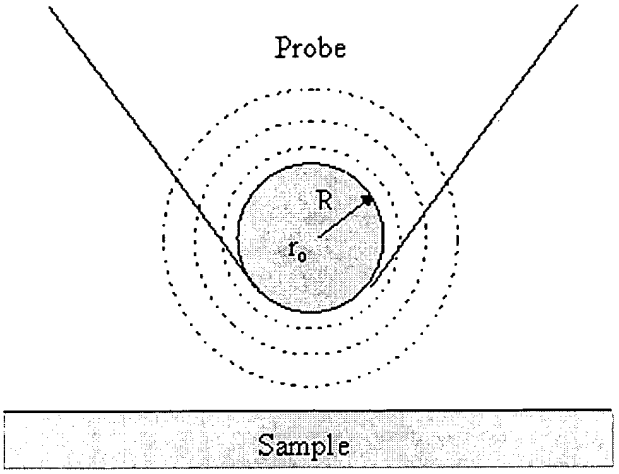

Figure 4

The s-wave probe model removes the probe interactions from the analysis in a way similar to the point source current model described earlier. Thus, the s-wave model reflects properties of the surface only.

Previous Section	Table of Contents	Next Section
Email Matt	Matt's Home Page	April 5, 1998

DESIGN AND CONSTRUCTION

The first scanning tunneling microscopes operated in ultra high vacuum, were equipped with sophisticated vibration isolation systems, and had minimal computer control. Early experimental work in controlled vacuum tunneling provided some of the groundwork for the first STM built by Binnig and Rohrer. Their first STM was a complicated design that operated in ultra high vacuum and used a primitive liquid helium suspension system for vibration isolation. Analog electronics generated the scanning waveforms and storage oscilloscopes recorded the topographic information. Since then, several designs using a combination of computer instrumentation and analog electronics have been tried but only a few designs have proven successful due to the constraints of STM operation.

Scanning a metal probe over a surface while maintaining a separation of a few angstroms requires very strict design parameters. Mechanical and acoustical vibration, electrical noise, and thermal drift are major impediments to the operation of an STM. For atomic resolution, the probe-sample separation, usually within 10 Å, must be controllable to less than .5 Å. The lateral resolution of the tunneling probe motion must be less than 1 Å. Creating this level of mechanical resolution in the lateral and vertical directions requires a system immune to vibration and thermal drift. The tunneling current measured by the STM is also exceedingly small. Generally, this current varies from several picoamps to a few nanoamps. Measuring currents at this level requires amplifiers with very high gain and noise immunity.

Advances in computer technology, data acquisition, and digital control systems enable the modern STM to be completely computer controlled. Computer control creates certain advantages as well as additional design constraints. The analog to digital (A/D) converters and the digital to analog (D/A) converters used in the computer control system must have high resolution and sufficient bandwidth to allow for reasonable scan acquisition times.

Even with the rigorous design constraints, scanning tunneling microscopes now routinely operate in a variety of conditions from cryogenic temperatures to 100° C and from ultra high vacuum to liquid environments. The STM designed here operates under computer control in an air environment. Figure 5 shows a block diagram of the system.

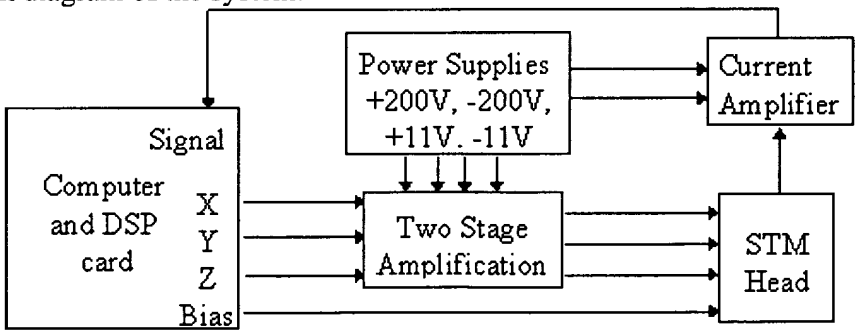

Figure 5

An IBM compatible computer with a digital signal processor (DSP) interface card generates the waveforms necessary for scanning. To drive the piezoelectric transducers in the STM head, a two stage amplification system provides a gain of approximately 10. A current amplifier reads the tunneling current from the STM head and then the DSP card digitizes this information. Three power supplies provide DC power for the piezoelectric amplifiers and the current amplifier.

Piezoelectric Transducers

Piezoelectric transducers are central to the operation of the STM. These transducers provide the finely controlled motion necessary for the demands of STM operation. No other motion control system (e. g. stepper motors) could operate with the precision of piezoelectric actuators.

Pierre Curie and his brother Jacques Curie discovered the piezoelectric effect in 1880. They discovered placing tension on a quartz plate sandwiched between two electrodes produces an electrical

charge. Not long after this discovery, Lippman predicted the inverse piezoelectric effect and again the Curie brothers experimentally investigated this phenomenon. In this experiment they used a light weight lever arm to magnify the displacement produced by applying a potential difference to a long piece of quartz sandwiched between two electrodes. The displacements produced by the inverse piezoelectric effect are very small. Thus, piezoelectric transducers are ideal positioners for scanning tunneling microscopes.[11]

Lead zirconate titanate (PZT) ceramics are the material used in the piezoelectric transducers of an STM. These materials change shape under an applied electric field. Figure 6 shows the behavior of a block of piezoelectric material under an applied electric field. By convention, the poling axis is defined to point from positive to negative. A piezoelectric material expands along the poling axis when a voltage is applied with the same polarity as the poling axis (V = +).

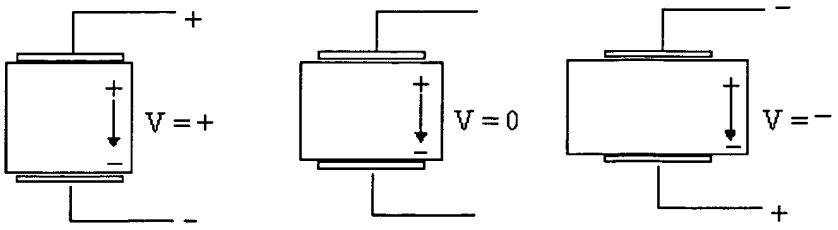

Figure 6

In the direction perpendicular to the poling axis, the material contracts. An applied field opposite to the poling axis (V = -) contracts the material parallel to the poling axis and expands the material perpendicular to the poling axis.[12]

The mechanism producing these displacements in PZT results from the ferroelectric nature of $PbZrO_3$ and $PbTiO_3$. In solid solution, these materials exhibit a permanent electric dipole even in the absence of an electric field. A ceramic solution of the two materials produces an isotropic material due to the random arrangement of the electric dipoles. Permanent polarization is produced by a poling process similar to that of making a permanent magnet from a hard ferromagnetic material. After a PZT is poled it can be used. Since piezoelectric ceramics are not single crystal materials, the anisotropic electric polarization produced by poling is not as stable or reproducible as the piezoelectric effect in single crystal materials such as quartz. Aging, hysteresis, depoling, and temperature sensitivity can change the electric polarization affecting PZT performance. Most PZT materials can be repoled by applying a suitable voltage at room temperature.[13]

The first scanning tunneling microscope used a tripod scanner arrangement similar to that in Figure 7. Three rectangular arms of piezoelectric material produced the

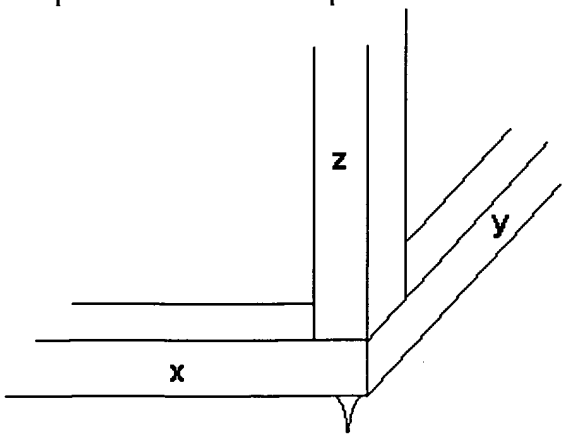

Figure 7

three orthogonal motions necessary for the STM. The length of the piezoelectric arm changes by ΔL equal to

$$\Delta L = \frac{d_{31} V L}{h}$$

when a voltage V is applied. In equation 18, h is the thickness of the material between the electrodes, L is the length of the rectangular piezoelectric arm, and d_{31} is the piezoelectric coefficient. This coefficient is defined as the ratio of the strain coefficient to the applied electric field (equation 19).

$$d_{31} = \frac{S_1}{E_3}$$

The standard convention labels the direction x, y, and z as 1, 2, and 3. Thus, d_{31} is the ratio of the strain in the x direction to the electric field applied in the z direction.

The mechanical design of the scanning tunneling microscope is directly related to the piezoelectric arrangement used to produce scanning motion. The STM must be insensitive to ambient vibrations and thermally stable as possible. These design constraints made the tripod scanner arrangement difficult to use for several reasons. First, the tripod arrangement was difficult to construct. Second, the physical dimensions of the tripod arrangement were large with low resonance frequencies that made the scanner susceptible to ambient vibration. Finally, obtaining calibrated motion in each direction was difficult due to variations in the piezoelectric material of each arm.

To solve some of the problems inherent in the tripod scanner design, Binnig and Smith developed the piezoelectric tube scanner (Figure 8).[14] Piezoelectric tube scanners generally have the tunneling probe mounted in a concentric fashion to one end of the tube. Bending the tube produces the scanning motion (x and y), and changing the

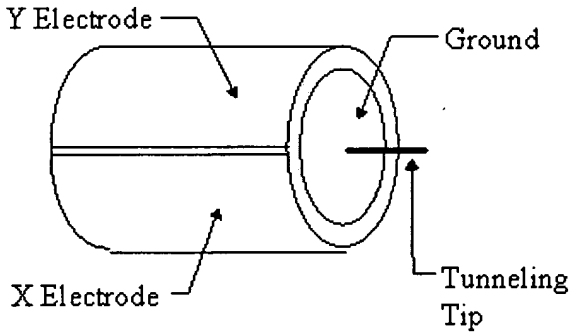

Figure 8

tube?s length creates the z motion for the scanner. The tube scanner has several advantages over the tripod scanner. Being one piece of piezoelectric material, the tube scanner is more rigid. Calibrating the deflection in each direction is easier since only one piezoelectric constant must be determined. Most importantly, the piezoelectric tube arrangement allows for the construction of very small scanning tunneling microscopes with high resonance frequencies.

The piezoelectric tubes used for scanning tunneling microscopes are poled radially usually with the outer electrode positive. With this arrangement, applying a negative voltage to all four quadrants of the tube while grounding the inner electrode expands the length of the tube by ΔL given by equation 18.

To create a horizontal deflection in the end of the tube, a voltage is applied to one of the quadrants while the other quadrants are grounded (Figure 9). This voltage changes the length of the corresponding quadrant of the tube creating a horizontal deflection in the

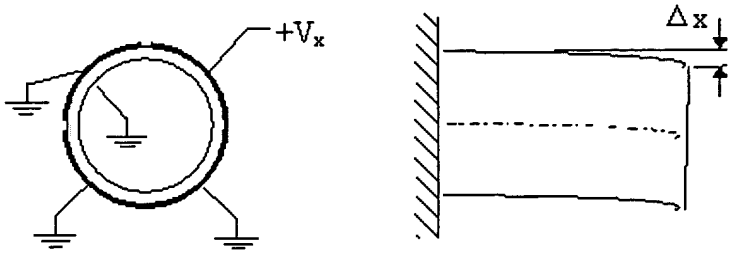

Figure 9

end of the tube. Equation 20 determines the amount of deflection.

$$\Delta x = \frac{\sqrt{2} d_{31} V L^2}{\pi D h}$$

V is the applied voltage, D is the diameter of the tube, L is the tube length, and h is the wall thickness of the tube. The sensitivity of a piezoelectric tube may be found by dividing both sides of equation 20 by V. Equation 20 also depends on the piezoelectric coefficient d_{31}, which is usually expressed in Å/V. Typical values for d_{31} range from -1.2 Å/V to -3 Å/V depending on the type of piezoelectric material.[15]

Applying voltages to only two of the four outer electrodes drives the piezoelectric tube in what is called the unipolar mode. The scan range, as well as the sensitivity of the piezoelectric tube, can be doubled in each direction (x and y) by operating the piezoelectric tubes in what is known as the bipolar mode. In this mode of operation, all four electrodes on the outside of the tube are used. A positive voltage is applied to one electrode and a negative voltage of the same magnitude is applied to the opposite electrode (Figure 10).

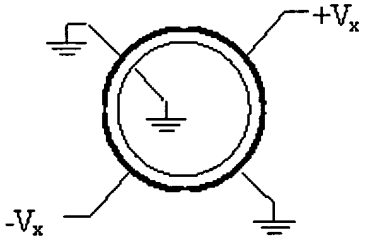

Figure 10

In the bipolar mode of operation, the applied voltage expands one side of the tube and contracts the other side of the tube. Thus, the end of the tube is deflected twice as much as the deflection produced in the unipolar mode. For the scanning tunneling microscope constructed here, the piezoelectric scanning tube is driven in the bipolar mode. The scanning tube has a diameter of 0.26 inches, a wall thickness of 0.025 inches and a length of one inch. The piezoelectric material of this tube has a d_{31} value of approximately -1.75 Å/V. Thus, the calculated sensitivity of the scanning piezoelectric tube is approximately 242.4 Å/V. The piezoelectric tube used to produce the z motion in this STM has a diameter of 0.48 inches, a wall thickness of 0.040 inches and a length of 1 inch giving the tube a calculated sensitivity of 43.4 Å/V.

The calculated value for the piezoelectric tube sensitivity may not correspond to the actual tube sensitivity for several reasons. For a given type of piezoelectric material, the piezoelectric coefficients are nominal values and vary for individual piezoelectric tubes. Furthermore, the piezoelectric coefficients may decrease if the material is handled improperly. Temperatures above the Curie point (>300 Celsius) and excessive electric fields, greater than 6kV/cm, applied opposite the poling direction may depole the material. As mentioned previously, since PZT materials are not single crystal, relaxation occurs in the material which also lowers the piezoelectric coefficients. This relaxation is logarithmic in nature and is measured in percent decrease per decade of time. Typical values for this relaxation vary from 0.5% to 6% per decade of time.

Determining the actual values of the piezoelectric coefficients can be done using a variety of

methods. Scanning a material with a known lattice size, such as highly oriented pyrolytic graphite (HOPG) can determine the d_{31} coefficient for the scanning tube. Other methods for calibrating piezoelectric constants include using an interferometer, a capacitive displacement sensor, or the double piezoelectric response[16] of the piezoelectric tube. Even after determining the d_{31} constant for a given piezoelectric tube, determining the actual displacement for a given voltage may still be difficult. Many piezoelectric materials suffer from hysteresis and creep effects. Furthermore, at high voltages the piezoelectric tubes do not respond linearly. Thus, at large deflection the actual displacement is difficult to determine.

Tunneling Probe

The condition of the tunneling probe is critical for obtaining atomic resolution. The first STM probe used a tungsten rod 1mm in diameter which was mechanically ground at an angle to produce a sharp probe.[17] Since then, many superior techniques have been developed for manufacturing probes for scanning tunneling microscopes. The most common method utilizes electrochemical etching. Etching the probe with a solution of potassium hydroxide (KOH) or sodium hydroxide (NaOH), produces probes with the properties important for scanning tunneling microscopy. The tunneling probes need an extremely small radius of curvature at the tip. Ideally, the probe needs atomic or near atomic sharpness. Also, the probes need to be short and rigid to prevent vibrations. Electrochemical etching produces very sharp probes. With this technique tungsten probes with radii or curvature of less than one micron can be produced.

The etching process also forms an oxide coating on the surface of the probe. This oxide prevents tunneling current from flowing, causing the probe to crash into the sample. The oxide must be removed prior to using the probe. Sophisticated methods, such as ion milling, have been developed to accomplish oxide removal; but most of these techniques only work in a vacuum. A simple solution to this problem is to gently crash the probe into the sample so that the oxide breaks, allowing current to flow.

Electrochemical etching of the tungsten rods is a simple procedure.[18] The first step is preparing the tungsten rod. The amount of etching current is proportional to the area of tungsten exposed to the solution. To minimize the etching current, the end of the rod is coated with shrink wrap. Maintaining a low etching current is essential. Higher current produces more bubbles at the etching surface. These bubbles make the etching uneven and can cause the lower portion of the tungsten rod to break off prematurely. After coating the end of the tungsten rod, it is lowered into a 1-2 M solution of NaOH or KOH in a 50 mL beaker until approximately 50-80 mA of current flows. At this current level a meniscus forms around the rod just above the heat shrink wrap. A variac provides an AC voltage of approximately 6 volts. When the etching is complete, the lower portion of the rod falls off, breaking the etching circuit. The usable probe is just above the surface of the solution. This method of preparation automatically shuts off the etching current as soon as the lower portion of the rod breaks away.

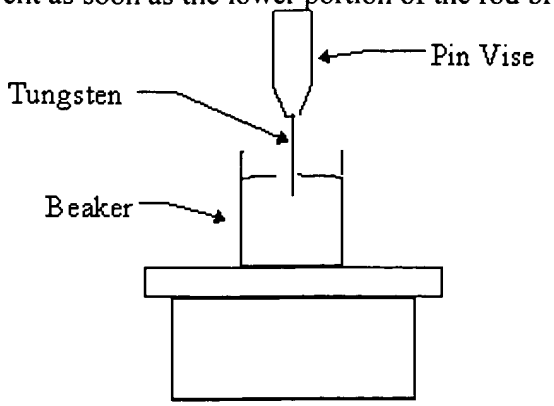

Figure 11

Producing a sharp probe depends on several factors, the most important being the time of etching

after the lower portion of the rod has fallen away. The procedure selectively etches away a small portion of the tungsten rod. Eventually the rod becomes so thin that the lower portion falls away. The etching current must be shut off as quickly as possible after the rod falls away to produce the sharpest probes. Several methods employing electronic circuits can automatically shut off the etching current; but, as mentioned previously, by etching the rod at the meniscus of the solution-air interface, the etching current is automatically shut off when the rod falls away.

Several tunneling probes have been produced with the aforementioned method. In some cases, the rod was positioned too low in the solution, resulting in the etching of the probe after the lower portion of the rod had fallen away. Under a scanning electron microscope, many of the probes produced appear to have a radius of curvature of less than 1 micron.

Previous Section	Table of Contents	Next Section
Email Matt	Matt's Home Page	April 5, 1998